Dielectric permittivity and AC conductivity in polycrystalline and amorphous C_{60}

J. Ortiz-López and R. Gómez-Aguilar
Instituto Politécnico Nacional, Escuela Superior de Física y Matemáticas,
Edif. 9, U.P.A.L.M.-Zacatenco, 07738 México D.F.,
e-mail: jortiz@esfm.ipn.mx

Recibido el 11 de febrero de 2003; aceptado el 26 de junio de 2003

The dielectric permittivity and AC conductivity of polycrystalline and amorphous C_{60} samples were measured at temperatures between 75 and 300 K and frequencies in the range 100 Hz to 1 MHz. For polycrystalline samples we observe effects caused by O_2 molecular oxygen intercalation because prolonged exposure to ambient air. The conductivity σ of these samples around 300 K depends on the measuring frequency ν as $\sigma \sim \nu^n$ with $n \approx 1$ implying a strong reduction of DC conductivity to less than 10^{-12} S/cm. Dielectric permittivity in polycrystalline samples shows an anomaly around 258 K due to its order-disorder phase transition and dielectric relaxation phenomena is observed in the range 130-200 K with an activation energy of 0.237 eV. In contrast with the polycrystalline samples, the amorphous C_{60} samples prepared by sublimation do not contain interstitial O_2, their DC conductivity at 300 K is of about 10^{-6} S/cm, is independent of frequency, and is well described by the hopping mechanism (Davis-Mott $T^{1/4}$ law) in the 200-300 K range. All evidence of phase transitions and/or dielectric relaxation disappears in the amorphous samples.

Keywords: Conductivity; dielectric permittivity and relaxation; fullerenes.

La permitividad dieléctrica y la conductividad AC de muestras policristalinas y amorfas de C_{60} se midieron a temperaturas entre 75 y 300 K con frecuencias en el intervalo de 100 Hz a 1 MHz. Para las muestras policristalinas observamos efectos debidos a la intercalación de oxígeno molecular O_2 por una prolongada exposición al aire ambiente. La conductividad σ de estas muestras alrededor de 300 K, depende de la frecuencia de medición ν como $\sigma \sim \nu^n$ con $n \approx 1$, implicando una fuerte reducción de la conductividad DC a menos de 10^{-12} S/cm. La permitividad dieléctrica en muestras policristalinas presenta una anomalía alrededor de 258 K debido a la transición de fase orden-desorden y, en el intervalo 100-200 K, se observan fenómenos de relajación dieléctrica con energía de activación de 0.237 eV. En contraste con las muestras policristalinas, las muestras C_{60} amorfas preparadas por sublimación no contienen O_2 intersticial, su conductividad DC a 300 K es de alrededor de 10^{-6} S/cm, es independiente de la frecuencia y queda bien descrita por el mecanismo de *hopping* (ley $T^{1/4}$ de Davis-Mott) en el intervalo 200-300 K. Toda evidencia de transiciones de fase y/o relajación dieléctrica desaparece en las muestras amorfas.

Descriptores: Conductividad; permitividad y relajación dieléctrica; fullerenos.

PACS: 72.20.Fr; 77.22.Gm; 77.22.Ch; 61.48.+c

1. Introduction

The C_{60} molecule is quasi-spherical with an effective radius of about 10 Å. In the solid state above 260 K, the molecules occupy sites of a cubic fcc lattice ($Fm\bar{3}m$) while rotating almost freely about their centers of mass. Below 260 K, solid C_{60} transforms into a simple cubic (sc) structure ($Pa\bar{3}$) with partial orientational order in which the molecules still perform hindered rotations between two orientations of minimal energy. With decreasing temperature, one of these orientations becomes gradually more populated, until a certain temperature is reached below which the relative populations remain constant (83% and 17%), therefore leaving the system in a state of frozen-in orientational disorder at low temperature [1, 2]. The establishment of this disordered state at low temperatures has been described as a 'glassy' transition occurring below a temperature T_g that depends on the characteristic time scale of the experimental technique of observation [1, 3].

Dielectric studies on C_{60} have been reported by several authors [4-10]. For C_{60} single crystals, Alers *et al.* [5] first reported that molecular orientational disorder in the sc ($Pa\bar{3}$) phase is manifested through dielectric relaxation phenomena. Since isolated C_{60} molecules do not have a permanent electric dipole because of their symmetry, the occurrence of dielectric relaxation was explained as due to induced electric dipole moments by adjacent pairs of misoriented molecules. Mondal *et al.* [6] working with polycrystalline samples confirmed that this dipolar relaxation is an intrinsic property of solid C_{60} and not due to defects or impurities. When comparing with results from experimental techniques probing C_{60} orientational dynamics at different time scales (dielectric, NMR, elastic, heat capacity, thermal conductivity, and thermal expansion), these authors concluded that C_{60} mean relaxation rates in the sc ($Pa\bar{3}$) phase follow an Arrhenius-type behavior for over 12 decades of measuring frequency [6], thus establishing the glass transition as a relaxational process.

The ease with which O_2 molecular oxygen from ambient air diffuses by hopping between octahedral interstitial sites of the C_{60} lattice is well documented [11-15]. In an initial stage of exposure to ambient air, a diffusion-controlled dielectric relaxation phenomena can be observed at room temperature because a small $O_2 - C_{60}$ charge transfer (~ 0.04e) causes a permanent electric dipole moment to appear. After prolonged exposure, all the interstitial sites become fully occupied, O_2 hopping is inhibited, and the room-temperature dipolar relaxation disappears [15]. The conductivity of an

oxygenated sample can be reduced up to six orders of magnitude in comparison to a pristine C_{60} sample because O_2 creates deep traps that effectively localize charge carriers [13]. Interstitial O_2 leaves essentially unchanged the crystalline structure of C_{60} and slightly reduces the ordering transition temperature [14]. Dielectric relaxation phenomena associated with molecular reorientations in the sc ($Pa\bar{3}$) phase is not precluded by oxygen intercalation [6].

In this work we perform dielectric measurements on C_{60} polycrystalline samples with prolonged exposure to ambient air, and on non-oxygenated amorphous samples obtained by rapid condensation of sublimated vapors. The oxygenated polycrystalline samples show essentially all features reported previously, that is, an anomaly in the real part of the dielectric constant at the fcc $\longrightarrow$ sc phase transition, dipolar relaxation in the sc phase, and a conductivity below 10^{-12} S/cm at room temperature. In the amorphous samples all manifestations of the phase transition disappear and the conductivity at room temperature is of the order of 10^{-6} S/cm. It is found that the conductivity for the amorphous samples in the 200-300 K range occurs by a hopping mechanism described by the Davis-Mott $T^{1/4}$ law.

2. Experimental details

Samples were prepared from 99.5 % pure C_{60} powder supplied by MER Corp. (Tucson, AZ, USA). For dielectric measurements, compressed pellets 0.2 - 0.3 mm thick and 6.3 mm diameter were prepared by applying no more than 0.3 ton of pressure with a hydraulic press. Electrodes were formed by applying silver paint or carbon conducting cement (Carbon Adhesive 30GM, Structure Probe, West Chester PA, USA) on both faces of the pellets. Less noisy samples were obtained with carbon cement electrodes. A group of samples, hereby named '$C_{60}-x$', were prepared from powders without any treatment. These powders had been exposed to ambient air for an undetermined amount of time so that their content of intercalated oxygen is considerable [15]. Another group of samples, to be called '$C_{60}-a$', were prepared from material obtained from the condensation of vapors when powders were sublimated at 700 °C inside a quartz tube under dynamic vacuum. These samples are evidently free of oxygen and due to the rapid condensation of vapors, exhibit a disordered structure. This is demonstrated by X-ray diffraction at room temperature (Siemens D500 diffractometer; $CuK_{\alpha 1}$ radiation, λ = 1.5405 Å) of the samples analyzed after dielectric measurements (electrodes included). In the diffraction patterns of Fig. 1, the total absence of Bragg peaks is clearly evident for $C_{60}-a$, justifying the classification of these samples as amorphous. In contrast, for $C_{60}-x$ the observed peaks can be indexed according to the expected fcc structure ($Fm\bar{3}m$) at room temperature with a lattice parameter $a = 14.18\mathring{A}$.

The capacitance C and conductance G of the samples were measured (in parallel mode) with an automatic impedance meter Hewlett-Packard HP-4284A operated in the 100 Hz to 1 MHz frequency range. The real and imaginary

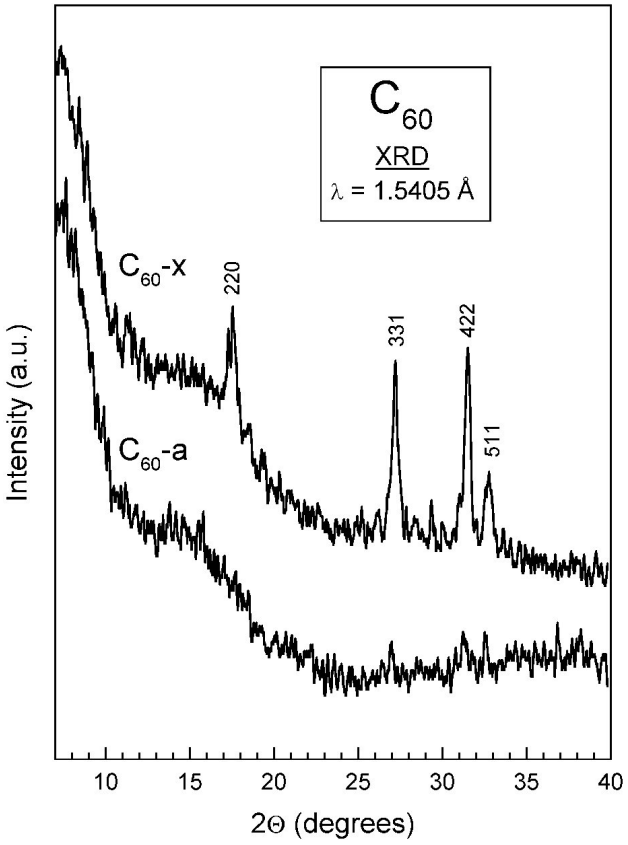

FIGURE 1. X-ray diffraction at room temperature of C_{60} polycrystalline ($C_{60}-x$) and amorphous ($C_{60}-a$) samples. Both patterns have the same scale but have been displaced vertically for clarity. For $C_{60}-x$ the observed peaks are indexed to a cubic fcc structure, *a* = 14.18 Å.

parts of the complex dielectric constant, ε' and ε'' respectively, are obtained from C and G according to: $\varepsilon' = C/C_0$ and $\varepsilon'' = G/\omega C_0$, where C_0 is the geometrical capacitance of the sample ($C_0 = \varepsilon_0 A/d$, where ε_0 is the permittivity of free space, *A* the area of electrodes and *d* the thickness of the sample), and $\omega = 2\pi\nu$, where ν is the measuring frequency. For materials having sizable conductivity it is convenient to express the imaginary part ε'' in terms of an AC conductivity defined as: $\sigma = (d/A)G = \varepsilon_0\omega\varepsilon''$. For good thermal contact with electrical insulation, the samples were placed between two sapphire disks in a sample holder designed to minimize mechanical and thermal stresses to the samples. Temperature was varied in the 75-300 K range with a cryostat (Janis 6DT) working with liquid nitrogen. Temperature control and measurement was performed with a Lake Shore 330 instrument coupled with a Si diode (DT-470) sensor. Data acquisition of C, G and temperature T was automated with the use of a PC.

3. Results

3.1. Polycrystalline C_{60} ($C_{60}-x$ samples)

For sample $C_{60}-x$ in Fig. 2 we present results of the real part of the dielectric constant ε' (which we abbreviate henceforth

simply as "dielectric constant") and of the conductivity σ as a function of temperature T and frequency ν. Our measurements for ε' at selected frequencies (10 kHz, 100 kHz and 1 MHz) are shown in Fig. 2a referred to the scale at the left. For comparison, we also include results reported by Alers *et al.* [5] in single crystals and by Mondal *et al.* in polycrystalline samples [6]. The former are referred to the scale at the left while the latter ones to the scale at the right. In our measurements, we observe under cooling that ε' weakly decreases at first but later, from about 258 K (we take this value as the critical temperature T_c) to about 240 K, ε' undergoes a frequency-independent increase with a relative change $\Delta\varepsilon'/\varepsilon' \approx 1.8\%$. The rapid increase of ε' in this temperature range is ascribed to the fcc $\longrightarrow$ sc phase transition in C_{60} [1,5,6]. At still lower temperatures, the ε' curves show a frequency-dependent gradual decrease (shoulder like) in the 130-200 K range (not very visible in the scale of Fig. 2a) which is due to the appearance of dielectric relaxation phenomena. These shoulders are correlated with (dielectric loss) maxima in ε'' or σ occurring in the same temperature range as we describe below. Finally, further cooling in the $75-130$ K range produces only a monotonous increase in ε'.

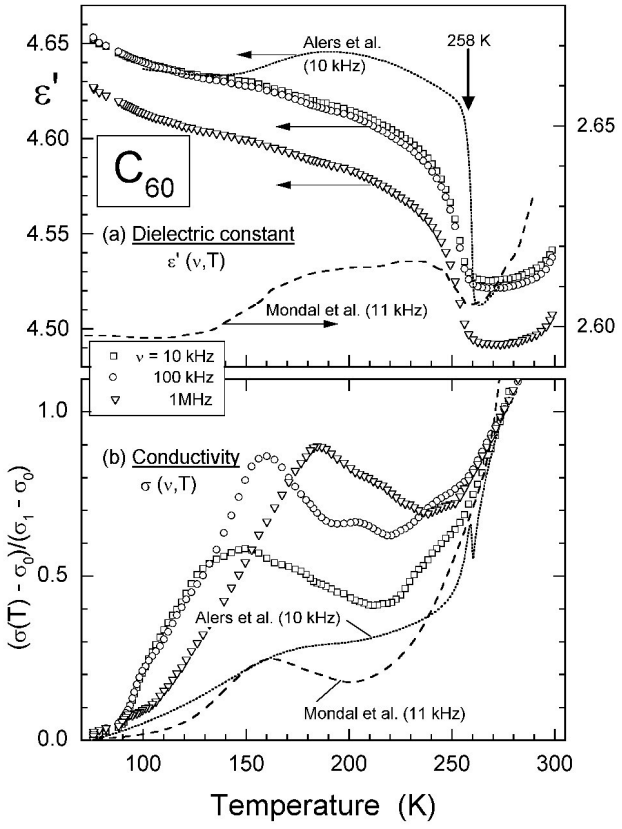

FIGURE 2. Temperature and frequency dependence of the real part of the dielectric constant $\varepsilon'(\nu,T)$ and of the conductivity $\sigma(\nu,T)$ for polycrystalline sample $C_{60}-x$. Data reported by Alers *et al.* [5] and by Mondal *et al.* [6] are also included. Note the distinct references to scales at left and right for $\varepsilon'(\nu,T)$ and the normalized scale used for $\sigma(\nu,T)$ (see text).

Our conductivity measurements for sample $C_{60}-x$ are presented in Fig. 2b. Because the measured $\sigma(\nu,T)$ depends strongly on frequency, and to avoid the use of confusing multiple scaling, we have plotted instead a normalized conductivity $[\sigma(\nu,T)-\sigma_0]/(\sigma_1-\sigma_0)$ in which σ_0 is the conductivity at T = 75 K, while σ_1 is the conductivity at T = 275 K. In our sample, σ_0 attains values of 1.713×10^{-9}, 1.745×10^{-8}, and 1.724×10^{-7} (S/cm) while σ_1 of 1.732×10^{-9}, 1.755×10^{-8}, and 1.732×10^{-7} S/cm at frequencies of 10 kHz, 100 kHz and 1 MHz, respectively. For comparison, in Fig. 2b we also present results of previously reported measurements [5, 6], both referred also to the same normalized scale. (Note that the original data of Ref. [6] are in terms of ε'' which we have converted to σ by using $\sigma = \varepsilon_0\omega\varepsilon''$). In our measurements towards high temperature, the curves show only a monotonous increase with no sign of an anomaly at the critical temperature 258 K. The most remarkable feature in Fig. 2b, however, is the appearance of (local) maxima in σ at frequency-dependent temperatures located within the same range (130-200 K) for which the shoulders are observed in our ε' data (Fig. 2a), and where dielectric relaxation has been reported earlier [5,6]. The maxima we observe in our data within the 130-200 K range, show similarities with those in Alers and Mondal *et al.* results, also depicted in Fig. 2b. Also note that the single crystal sample of Alers *et al.* shows clearly an anomaly in σ around the critical temperature (~ 260 K), while for polycrystalline samples, like Mondal's and ours, this anomaly is washed out.

3.2. Amorphous C_{60} ($C_{60}-a$ samples)

In Fig. 3 we present for sample $C_{60}-a$, the temperature dependence of ε' and σ (in logarithmic scale) at different frequencies. The behavior displayed by $C_{60}-a$ is notoriously different from that observed in polycrystalline $C_{60}-x$ (Fig. 2). There is no sign whatsoever of any anomaly in ε' or σ at the critical temperature 258 K that we measured in the polycrystalline sample. At high temperatures in $C_{60}-a$, ε' is characterized by a strong frequency dependence (dispersion) and attains particularly large values at low frequencies. On cooling, ε' and σ decrease monotonously in such a way that the dispersion in ε' gets reduced, while the σ curves approach constant values that depend on frequency.

4. Discussion

4.1. Polycrystalline C_{60} ($C_{60}-x$ samples)

Our results for ε' in $C_{60}-x$ are in good general agreement with those reported in previous publications. The value $\varepsilon' = 4.54$ that we obtain in this work for C_{60} at room temperature is in good accord with other reported values, for example: ε' in the range 4.0-4.5 obtained by ellipsometry and optical reflectance/transmittance in thin films [16], $\varepsilon' = 4.4$ from dielectric measurements in thin films [4] and single crystals [5] and, $\varepsilon' = 4.6$ obtained from EELS [17]. Nevertheless,

certain discrepancies are found, particularly in comparison with the results of Mondal *et al.* [6], who ambiguously report two different values $\varepsilon' \approx 2.6$ and 3.3 at room temperature, which they obtain from the same measurement published in two different journals within a period of two years. To compare in more detail our results with previous work, in Table I we present a comparison of some parameters that characterize the temperature dependence $\varepsilon'(T)$ of C_{60}. We choose to compare our results with those from Alers *et al.* [5], Mondal *et al.* [6], and Min Gu *et al.* [7] because their results are the most comprehensive ones we have found in the literature. Among these, the most dissimilar ones are those of Min Gu who report a complicated behavior around T_c, with the peculiarity that ε' displays a peak in T_c only in measurements under heating (such behavior was never observed in our case). Other distinct feature of Min Gu's results is that they are the only ones that show a positive slope $\partial\varepsilon'/\partial T$ for the background dielectric response. On the other hand, the measurements of Alers et al. in single crystals and of Mondal *et al.* in polycrystals, are in better agreement with our results. In single crystals, the transition occurs within a narrow temperature range ($\sim$ 6 K) while in polycrystals, the transition is more sluggish and spreads over a wider temperature range ($\sim$ 24 K). This effect has also been observed previously in heat capacity measurements [18].

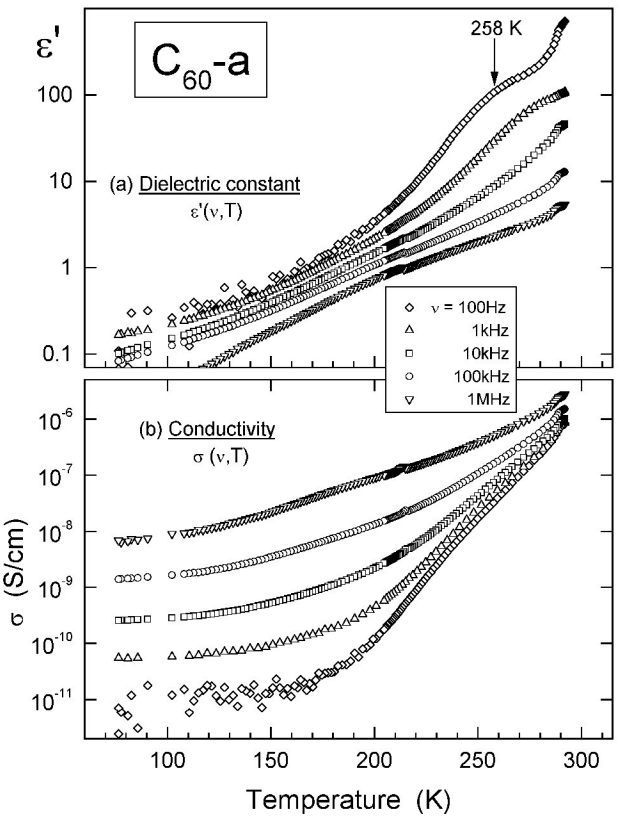

FIGURE 3. Temperature and frequency dependence of the real part of the dielectric constant $\varepsilon'(\nu, T)$ and of the conductivity $\sigma(\nu, T)$ for amorphous sample $C_{60}-a$. No anomalies due to phase transitions are detected at 258 K.

The relative size of the anomaly in ε' at T_c that we measure in this work for polycrystalline $C_{60}-x$, turns out to be considerably larger than the one measured previously also in polycrystals [6], and only slightly smaller than the one found in single crystals [5]. For dielectric relaxation in the temperature range 130-200 K, the relative size of the 'relaxation step' (or shoulder in ε', Fig. 2a) is in fair agreement with the one obtained by Alers and Mondal *et al.* Discrepancies between our results and those of other authors can be expected to occur because of variations in experimental conditions and instrumentation. These may be caused, for example, by the use of different type of measuring apparatus or by temperature dependent variations of stray capacitance due to thermal contraction of sample holder and surroundings. Nonetheless, we must still consider an additional reason that could even be more significant. The $C_{60}-x$ sample was prepared from powder that stood exposed to ambient air for prolonged time. It is well known that molecular oxygen O_2 from ambient air diffuses reversibly and with great ease in solid C_{60} occupying and hopping between octahedral interstitial sites of its fcc lattice [11-15]. It has also been found that a charge transfer occurs between O_2 and C_{60} molecules that can give rise to dielectric relaxation even at room temperature [15]. This room-temperature dielectric relaxation disappears after all the available interstitial sites become occupied by O_2 after prolonged air exposure. It is then clear that our $C_{60}-x$ sample is in an oxygenated state and this condition must be taken into account in the discussion. In the case of Mondal *et al.* [6], they carefully removed interstitial oxygen from their samples by annealing (at 750 K) in vacuum several times. Alers *et al.* [5] are not so explicit but we are certain they were careful enough not to expose their samples to air for a long time after growing their single crystal samples. Therefore, our samples and those of Alers and Mondal *et al.* differ in terms of their content of interstitial oxygen. This oxygenation affects in various ways the properties of solid C_{60}. In particular, it is well known that lattice phonons as well as the dynamics of molecular ordering and reorientation are perturbed by interstitial O_2 [11, 19]. This could well be the origin of the differences found with our results in Table I; in particular, this explains why T_c in our sample $C_{60}-x$ is displaced downwards to 258 K. Other important aspect of oxygenation is the creation of deep level traps for charge carriers [12,13,15,19], which can affect drastically the electrical conductivity.

When the conductivity is measured with an AC technique of frequency $\omega = 2\pi\nu$, the response that characterizes a great variety of materials with diverse chemical compositions, either crystalline or amorphous, can be written as [20]

$$\sigma(\omega, T) = \sigma_{DC}(T) + a(T)\omega^n, \qquad (1)$$

where $\sigma_{DC}(T)$ is the 'direct current' (or static, $\omega = 0$) conductivity, *a*(T) is a factor that depends on temperature but not on ω, and *n* is an exponent in the range $0.6 \leq n \leq 1$. Equation (1) predicts that if (at certain temperature) σ_{DC} is much less than the second term, then $\sigma(\omega, T) \propto \omega^n$, so that a log-log plot of σ against ω describes a straight line with slope *n*.

TABLE I. Comparison of results for $\varepsilon'(T)$ in sample $C_{60} - x$ with those reported in other publications.

	this work (polycrystal)	Alers [5] (single crystal)	Mondal [6] (polycrystal)	Min Gu [7](polycrystal)
Onset of transition, T_c [K]	258 (cooling)	260 (cooling)	260 (cooling)	245 (cooling) 252 (heating)
Width of transition, ΔT [K]	24	6	25	22 (cooling) 20 (heating)
Anomaly at T_c, $\Delta\varepsilon'/\varepsilon'$ in %	1.8	2.4	0.4	0.3 (jump, cooling) 1.7 (peak, heating)
Relaxation step, $\Delta\varepsilon'/\varepsilon'$ in %	0.45±0.10	0.60±0.10	0.57±0.10	No data is presented
Background slope, $\frac{\partial\varepsilon'}{\partial T}$ $[K^{-1}]$	-5.24 × 10^{-4}	-1.82×10^{-4}	-1.24×10^{-5}	+6.67×10^{-5}

On the other hand, if σ_{DC} becomes larger than the second term (by increasing temperature, for example), then $\sigma(\omega, T) \propto \sigma_{DC}(T)$, in which case the AC technique renders a measurement of σ_{DC}, and a plot of σ against ω in log-log scale should give a horizontal straight line. The behavior of $\sigma_{DC}(T)$ for polycrystalline semiconductors, is usually interpreted in terms of Seto's grain boundary trapping theory [21], which assumes the presence of a large amount of trapping states at the grain boundary able to capture free carriers. These (charged) states at grain boundaries create potential barriers, which oppose the passage of carriers from a grain to the neighboring ones.

When plotting in Fig. 4 our data of σ against $\nu(=\omega/2\pi)$ in log-log scale for sample $C_{60} - x$, we clearly observe a linear behavior implying a negligible contribution of $\sigma_{DC}(T)$ according to Eq. (1). The best fit to the data gives *n* = 1.007 for a wide temperature range (125-300 K). From careful examination of Fig. 4 we can deduce that $\sigma_{DC} \leq 10^{-12}$ S/cm, because σ_{DC} should be smaller than the minimum value of σ measured at the lowest frequency (100 Hz). This is in good agreement with the strong reduction of conductivity expected from the oxygenation of our sample [13, 15, 19].

Finally, in Fig. 5 we analyze the dielectric relaxation observed in the $130 - 200$ K range for sample $C_{60}-x$. Relaxation of a dipolar system is usually a thermally activated process if temperatures are not too low. The relaxation rate ν is related to the relaxation time τ by $\nu = (2\pi\tau)^{-1}$ and has a temperature dependence given by

$$\nu(T) = \nu_0 \exp\left(-\frac{U}{k_B T}\right), \qquad (2)$$

where ν_0 is the "attempt frequency", *U* the reorientation barrier, k_B is Boltzmann's constant and *T* is the absolute temperature. Figure 5 is an Arrhenius-type plot of the measuring frequency ν against the inverse of the temperature position of the (local) maxima observed in σ in the 130-200 K range (Fig. 2b). A reasonable fit to the behavior of Eq. (2) is achieved with $\nu_0 = 2.4 \times 10^{12}$ Hz and *U* = 0.237 eV. In Fig. 5 we have also included results from Alers *et al.* [5] and Mondal *et al.* [6] for two of the samples each group reports, and also a global mean value (marked as Mondal-tot) that Mondal gives as the best fist to data obtained from a variety of techniques covering about 13 decades in frequency. The reorientation parameters obtained by these authors are compared in Table II against our results. We find a fair agreement with the reported results but we note that our value for *U* is a bit smaller. This reduction in reorientation barrier is again a consequence of the oxygenation of our sample $C_{60}-x$. The small charge transfer between O_2 and C_{60} molecules [15] as well as the expansion that O_2 must cause to the C_{60} lattice [11] are effects that contribute to the reduction of reorientational barriers.

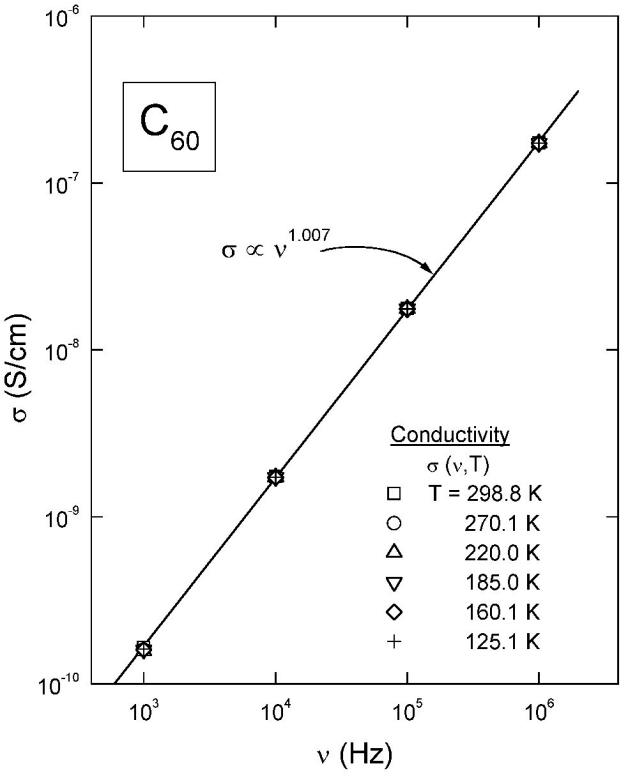

FIGURE 4. Log-log plot of the conductivity $\sigma(\nu, T)$ against frequency ν in sample $C_{60}-x$ for temperatures in the range 125-300 K.

TABLE II. Comparison between molecular reorientation parameters obtained in sample $C_{60}-x$ with those reported in other publications.

	$\nu_0[Hz]$	U[eV]
This work	2.4×10^{12}	0.237
Alers *et al.* [5]	1) 1.6×10^{12}	1) 0.270
	2) 7.9×10^{12}	2) 0.280
Mondal *et al.* [6]	1) 2.0×10^{13}	1) 0.293
	2) 8.0×10^{13}	2) 0.306
	tot) 2.4×10^{13}	tot) 0.296

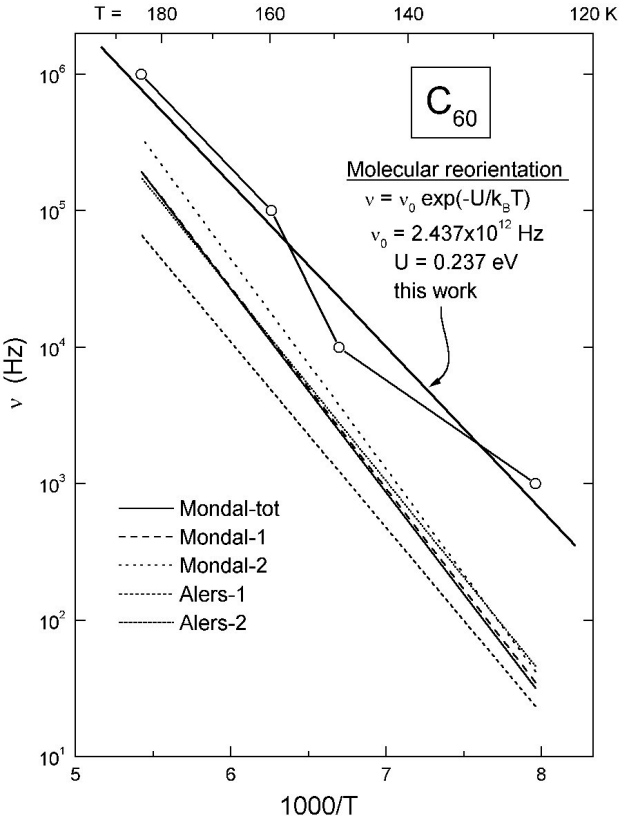

FIGURE 5. Arrhenius-type plot for the molecular reorientation rate in sample $C_{60}-x$. Data reported by Alers *et al.* [5] and by Mondal *et al.* [6] are also included.

4.2. Amorphous C_{60} ($C_{60}-a$ samples)

The description of samples $C_{60}-a$ as amorphous (supported by X-ray diffraction in Fig. 1) is confirmed by the inexistence of anomalies in ε' due to phase transitions in the results of Fig. 3. Considering that these samples are obtained from the rapid condensation of sublimated vapors, they should consist of C_{60} molecules rotating freely around their centers of mass occupying sites deprived of translational symmetry. The disorderly positions of neighbors around a given C_{60} molecule prevent collective coupling of interactions that affect their rotational motion and, in consequence, the ordering transition occurring at 260 K in crystalline C_{60} no longer takes place. Due to this structural disorder, it is also expected that the dielectric relaxation phenomena observed in crystalline C_{60} in the 130-200 K range is also prevented.

The strong dispersion observed in Fig. 3 for $C_{60}-a$ is evidenced by large room-temperature values for $\varepsilon'(\approx 716)$ at low frequency (100 Hz). This behavior in the dielectric response is similar to the so called Maxwell-Wagner effect [20] which is usually interpreted as due to interfacial polarization as occurs when, for example, blocking contacts are established. However, this behavior can also be observed in heterogeneous systems like granular materials or in systems where exist barriers and traps to the transport of charge carriers, as it occurs in amorphous materials.

Our conductivity data in Fig. 3 for $C_{60}-a$ show notorious contrast with that obtained for polycrystalline $C_{60}-x$ (Fig. 2). The plot in Fig. 6 for the frequency dependence of σ in $C_{60}-a$ at different temperatures should be compared to the equivalent plot for $C_{60}-x$ in Fig. 4. From this comparison it is clear that for $C_{60}-a$, the conductivity at room temperature is basically independent of frequency and, according to Eq. (1), the measurement of σ (at low frequency) is equivalent to $\sigma_{DC}(T)$, at least in the 250-300 K range. With decreasing temperature, σ_{DC} becomes smaller and the second term in Eq. (1) starts to dominate. In this regime, a fit to the data gives $\sigma \propto \nu^n$ with n = 0.72. Also from Fig. 6 we

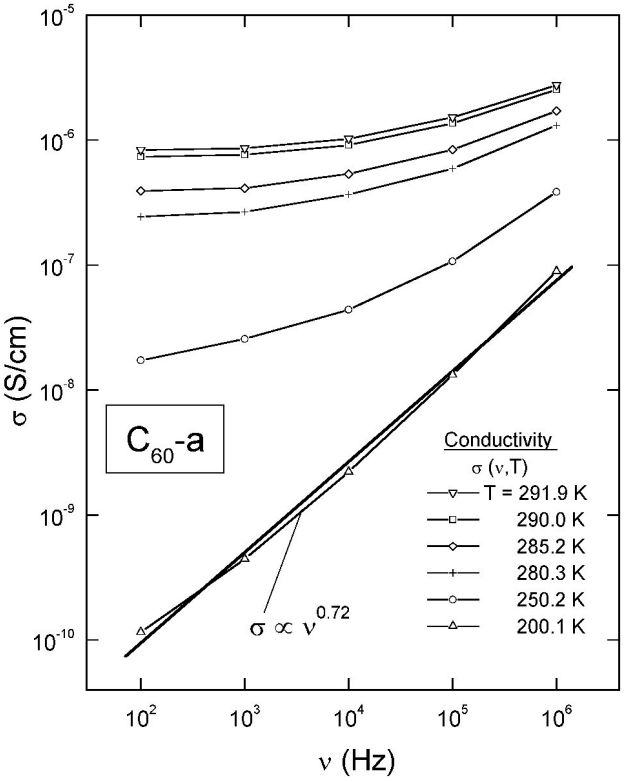

FIGURE 6. Log-log plot of the conductivity $\sigma(\nu, T)$ against frequency ν in sample $C_{60}-a$ for temperatures in the range 200-300 K.

can assert that $\sigma_{DC} \approx 10^{-6}$ S/cm for $C_{60}-a$ at room temperature, which should be compared with $\sigma_{DC} \leq 10^{-12}$ S/cm, as already discussed for polycrystalline sample $C_{60}-x$. Six orders of magnitude reduction in conductivity is the result of prolonged air exposure of sample $C_{60}-x$.

According to the Davis-Mott model for amorphous semiconductors, the standard energy band scheme describing a crystalline material changes in the amorphous case so that the valence and conduction bands stretch out and develop 'tails' while a middle allowed band (compensated levels) also shows up near the center of the forbidden band gap [22, 23]. Carriers with energies within the tails and the central band are described by localized states while for other energies, the carriers are in extended states. In the Davis-Mott model, there are three mechanisms of charge transport that dominate over different temperature ranges:

(i) at the highest temperatures, the carriers are excited into extended states where they acquire mobilities orders of magnitude greater than in localized states;

(ii) at medium temperatures, the carriers are excited into localized states in the valence and conduction band tails; and

(iii) at the lowest temperatures, conduction occurs by tunneling between states located in the central band near the Fermi level.

For case (i), the temperature dependence of $\sigma_{DC}(T)$ predicted by this model is Arrhenius-type (thermally activated) with an activation energy that equals the difference between the Fermi level and the energy that defines the boundary between localized and extended states. In case (ii), conduction occurs by thermally activated hopping and $\sigma_{DC}(T)$ also is of Arrhenius-type behavior but with an activation energy that involves the Fermi level, the energies of the tail edges, and a hopping activation energy, and in addition, the pre-exponential factor acquires a weak temperature dependence. Finally for case (iii), conduction is by phonon-assisted tunneling, also known as 'variable-range hopping' and in that case $\sigma_{DC(T)}$ can be written as

$$\sigma_{DC}\,(T) = \frac{\sigma_0}{\sqrt{T}} \exp\left[-\left(\frac{T_0}{T}\right)^{\frac{1}{4}}\right], \qquad (3)$$

where σ_0 and T_0 are parameters of Davis-Mott model [22, 23].

Information about $\sigma_{DC}(T)$ extracted from our data for $C_{60}-a$ has been analyzed in terms of the three mechanisms (i)-(iii) of the Davis-Mott model mentioned above. Our analysis indicates that the data is best described by mechanism (iii) as can be seen in Fig. 7 where a fit to the behavior given by Eq. (3) is reasonably good for temperatures in the range 200-300 K, covering a range of about four decades in conductivity. The adjusting parameters are: $T_0 = 2.022 \times 10^{10}$ K and $\sigma_0 = 4.416 \times 10^{34} K^{1/2}$S/cm. In conclusion, DC conductivity in sample $C_{60}-a$ is well described by a (variable-range) hopping mechanism in the 200-300 K temperature range.

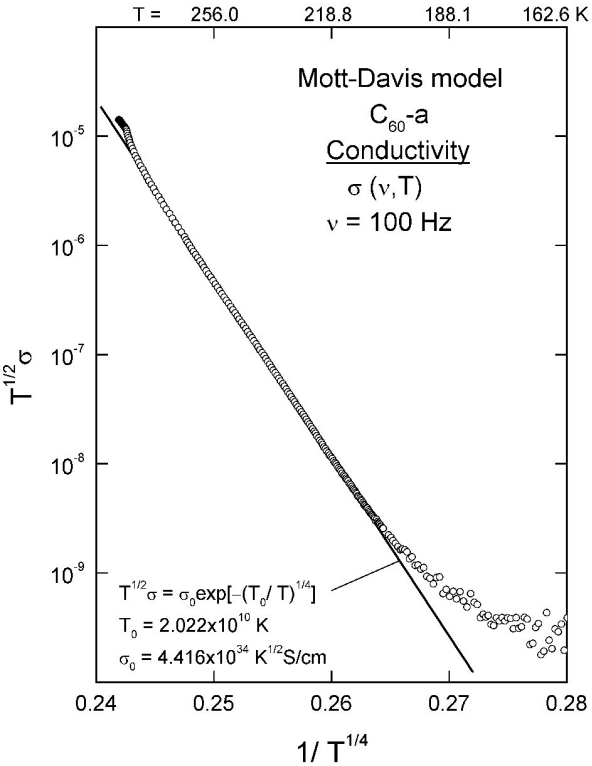

FIGURE 7. Data of direct conductivity $\sigma_{DC}(T)$ fitted to the Mott-Davis model in sample $C_{60}-a$ ($\nu = 100$ Hz).

5. Conclusions

The dielectric constant ε' and conductivity σ of polycrystalline and amorphous samples of C_{60} were measured in the 75-300 K temperature range at frequencies between 100 Hz and 1 MHz.

Prolonged exposure to ambient air of the material employed in the preparation of polycrystalline samples drastically affects charge transport but weakly perturbs their dielectric properties. Occupation of interstitial sites of C_{60} lattice by molecular oxygen O_2, does not change the crystalline structure or quenches interactions responsible for molecular ordering, but effectively creates traps for charge carriers. In polycrystalline C_{60}, DC conductivity at room temperature becomes less than 10^{-12} S/cm as a result of oxygenation. For samples prepared by sublimation and rapid condensation, their amorphous nature is confirmed in dielectric measurements by the total absence of phase-transition anomalies in the measured dielectric constant. Because amorphous samples are oxygen-free, their DC conductivity at room temperature turns out to be of 10^{-6} S/cm, that is, six orders of magnitude higher than the oxygenated polycrystalline samples. DC conductivity in the amorphous samples is well described in the 200-300 K range by Mott-Davis variable-range hopping model.

Acknowledgments

One of us (J.O.L.) gratefully acknowledges partial support from CONACYT (México) grant Nos. F143-19201 and F-596-E9404, to CGPI-IPN for support to Projects Nos. 20010558 and 20020911, and to COFAA-IPN for a SIBE fellowship.

1. P.A. Heiney *et al.*, *Phys. Rev. Lett.* **66** (1991) 2911; J.E. Fischer and P.A. Heiney, *J. Phys. Chem. Solids* **54** (1993) 1725.
2. W.I.F. David, R.M. Ibberson, T.J.S. Dennis, J.P. Hare, and K. Prassides, *Europhys. Lett.* **18** (1992) 219.
3. T. Matsuo *et al.*, *Solid State Commun.* **83** (1992) 711.
4. A.F. Hebard, R.C. Haddon, R.M. Fleming, and A.R. Kortan, *Appl. Phys. Lett.* **59** (1991) 2109.
5. G.B. Alers, B. Golding, A.R. Kortan, R.C. Haddon, and F.A. Theil, *Science* **257** (1992) 511.
6. P. Mondal, P. Lunkenheimer, R. Bohmer, A Loidl, F. Gugenberger, P. Adelmann, and C. Meingast, *J. Non-Crystalline Solids* **172-174** (1994) 468; P. Mondal, P. Lunkenheimer, and A. Loidl, *Z. Phys. B.* **99** (1996) 527.
7. Min Gu, Y. Wang, T.B. Tang, F. Yan, H. Zhou, W. Zang, P. Yang, and J. Zhu, *J. Phys.: Condens. Matter* **6** (1994) 8871.
8. G. Chern, H. Mathias, L.R. Testardi, L. Seger, and J. Schenloff, *J. of Superconductivity* **8** (1995) 207.
9. F. Yan and Y.N. Wang, *Appl. Phys, Lett.* **72** (1998) 3446.
10. J.B. Shi, *Physica B* **284-288** (2000) 1131.
11. Z. Belahmer, P. Bernier, L. Firlej, J.M. Lambert, and M. Ribet, *Phys. Rev. B* **47** (1993) 15980.
12. A. Hamed, Y.Y. Sun, Y.K. Tao, R.L. Meng, and P.H. Hor, *Phys. Rev. B* **47** (1993) 10873.
13. C.H. Lee, G. Yu, B. Kraabel, D. Moses, and V.I. Srdanov, *Phys. Rev. B* **49** (1994) 10572.
14. M. Jaime and M. Nunez Regueiro, *Appl. Phys. A* **60** (1995) 289.
15. B. Pevzner, A.F. Hebard, and M.S. Dresselhaus, *Phys. Rev. B* **55** (1997) 16439.
16. Y. Wang *et al.*, *Phys. Rev. B* **45** (1992) 14396.
17. P.L. Hansen, P.J. Fallon, and W. Kratschmer, *Chem. Phys. Lett.* **181** (1991) 367.
18. Y. Miyazaki, M. Sorai, R. Lin, A. Dworkin, H. Szwarc, and J. Godard, *Chem. Phys. Lett.* **305** (1999) 293.
19. M.S. Dresselhaus, G. Dresselhaus, and P.C. Eklund, *Science of Fullerenes and Carbon Nanotubes* (Academic Press, 1996).
20. A.K. Jonscher, *Dielectric Relaxation in Solids* (Chelsea Dielectric Press, London, 1983).
21. J.Y.W. Seto, *J. Appl. Phys.* **46** (1975) 5247.
22. P. Nagels, *Electronic Transport in Amorphous Semiconductors, Topics in Applied Physics, Amorphous Semiconductors, M.H. Brodsky editor* (Springer-Verlag, 1979).
23. N.F. Mott and E.A. Davis, *Electronic Processes in Non-Crystalline Materials*, 2nd ed. (Clarendon, Oxford, 1979).